

A simple analytical EAM model for some bcc metals

Ibrahim H. Dursun^{a,1}, Ziya B. Güvenç^{b,*}, E. Kasap^c

^a Faculty of Science and Literature, University of Aksaray, TR-68100 Aksaray, Turkey

^b Electronic and Communication Engineering, Cankaya University, TR-06500 Balgat Ankara, Turkey

^c Faculty of Science and Literature, Gazi University, TR-06500 Ankara, Turkey

ARTICLE INFO

Article history:

Received 18 April 2009

Received in revised form 8 May 2009

Accepted 9 May 2009

Available online 19 May 2009

PACS:

31.15.xv

61.43.Bn

61.66.Dk

61.50.-f

62.20.-x

Keywords:

Alloys

Surface

Impurity

Molecular Dynamics Simulation (MDS)

Embedded Atom Method (EAM)

Heat capacity

Under-cooled

Specific heat

bcc metals

ABSTRACT

An analytical embedded atom method which can treat bcc transition metal iron has been developed. In this model, a new potential was proposed and a modified term has been introduced to fit the negative Cauchy pressure $P_C = (C_{12} - C_{44})/2$ for Fe element. The new model was applied to calculate thermodynamic properties of binary alloys of the bcc transition metals; Fe, V and Cr. The calculated dilute solution enthalpies and formation enthalpies of random alloys are in good agreement with the results of first principles calculations and that of the thermodynamic calculations.

© 2009 Elsevier B.V. All rights reserved.

1. Introduction

Daw and Baskes [1] derived so-called Embedded Atom Method (EAM) on the basis of quasi-atom concept and density-function-theory. Since then, the semi-empirical theory attracts great interest of scientists in materials science and condensed matter physics. It has been applied successfully to metals, impurity, surface, alloys, liquids and mechanical properties [1,2].

Johnson [3] proposed an analytical EAM model, this model was applied to calculate the thermodynamic properties for binary alloys of the bcc transition metals; Fe, V and Cr by Johnson and Oh [4], Bangwei and Yifang [5], however, the model cannot treat transition metal, iron, for its negative Cauchy pressure $P_C = (C_{12} - C_{44})/2$. Then, Pasianot et al. [6] proposed a so-called embedded defect potential, which can fit the negative Cauchy pressure of iron.

* Corresponding author. Tel.: +90 312 2844500.

E-mail addresses: hidursun@aksaray.edu.tr (I.H. Dursun), guvenc@cankaya.edu.tr (Z.B. Güvenç), ergun@gazi.edu.tr (E. Kasap).

¹ Tel.: +90 382 2151654.

At this point, the model of Pasianot et al. [6] is successful, but the model, on the one hand, has a complex expression, especially, the modified term was not given clearly, on the other hand, the model has not been tested for other applications. So their model needs to be tested extensively. Adams and Fopiles [7] proposed an EAM model for metal Vanadium (V), the model is not analytical.

In this paper, we present a new pair potential. In order to fit the negative Cauchy pressure, an analytic modified term $M(P)$ has been introduced. The developed analytical EAM model has been applied to calculate the self-diffusion properties of the bcc transition metals [5]. The results are in good agreement with the available experimental values. In the present work this model was applied to calculate the dilute-solution enthalpies and formation enthalpies of binary alloys of the bcc transition metals; Fe, V and Cr.

2. Model

The EAM is one of the distinguished potentials which gains great success in describing the interaction of particles of metals and alloys. It has been shown to give good results in simulations of reconstructions, thermal expansion, surface and liquid structure, and even for the under-cooled liquid-to-glass and liquid-to-crystalline transitions. The EAM is a procedure for designing a mathematical model of a metal which was developed by researchers at Sandia National Laboratory, from the EAM the total energy of an assembly of atoms is [1]

$$E_t = \sum_i F_i(\rho_i) + \frac{1}{2} \sum_{i \neq j} \phi(r_{ij}) \quad (1)$$

$$\rho_i = \sum_{j \neq i} f(r_{ij}) \quad (2)$$

where E_t is the total internal energy, ρ_i is the electron density at i due to all the other atoms, $f(r_{ij})$ is the electron density distribution function of an atom, r_{ij} is the separation distance between atom i and atom j , $F(\rho_i)$ is the embedding energy to embed atom i into an electron density ρ_i , and $\phi(r_{ij})$ is the two-body potential between atom i and atom j . Following the previous procedure of EAM, the negative Cauchy pressure cannot be fitted. So in the present model an analytical modified term $M(P_i)$ has been introduced. Then (1) is written in the following form:

$$E_t = \sum_i F_i(\rho_i) + \frac{1}{2} \sum_{i \neq j} \phi(r_{ij}) + \sum_i M(P_i) \quad (3)$$

$$P_i = \sum_{j \neq i} f^2(r_{ij}) \quad (4)$$

The modified term $M(P_i)$ is based on two reasons. One is from (2), the total electron density at the position of atom i is the superposition of contribution from all the other atoms, this assumption is too simple and neglects the hybridization and the polarity. The other is the spherical symmetric assumption of electron density distributions. In fact, the outer electron density distribution is not spherically symmetric except the s-electron. The modified term $M(P_i)$ represents the discrepancy between the assumptions, and the facts. According to Johnson and Oh's procedure of development of the EAM [3], the potential function satisfies the following equations:

$$4\phi(r_1) + 3\phi(r_2) = -E_{1f} \quad (5)$$

$$4\phi'(r_1) + 3\phi'(r_2) = 0 \quad (6)$$

$$4\phi''(r_1) + 3\phi''(r_2) = 15\Omega G \quad (7)$$

$$\frac{8(r_1^2\phi''(r_1) - r_1\phi'(r_1))}{9(r_2^2\phi''(r_2) - r_2\phi'(r_2))} = A \quad (8)$$

The embedding function and the modified term satisfy the following equations:

$$F(\rho_e) = -F_0 \quad (9)$$

$$F'(\rho_e) = 0 \quad (10)$$

$$F''(\rho_e) \frac{(8r_1 f'(r_1) + 6r_2 f'(r_2))^2}{(8f(r_1) + 6f(r_2))^2} + M''(P_e) \frac{4(8r_1 f(r_1) f'(r_1) + 6r_2 f(r_2) f'(r_2))^2}{(8f^2(r_1) + 6f^2(r_2))^2} = 9\Omega B - 15\Omega G \quad (11)$$

$$M(P_e) = 0 \quad (12)$$

$$M'(P_e) = 0 \quad (13)$$

where E_{1f} is the mono-vacancy formation energy, r_1 and r_2 are the nearest and next-nearest neighbor distances, respectively, the prime indicates differentiation to its argument. The Ω is the equilibrium volume of an atom, G is the Voigt shear modulus, $G = (C_{11} - C_{12} + 3C_{44})/5$, C_{11} , C_{12} and C_{44} are elastic constants, A is the anisotropic ratio, $A = 2C_{44}/(C_{11} - C_{12})$, B is the bulk modulus, ρ_e is the equilibrium value of the total electron density ρ , P_e is the equilibrium value of P , F_0 is the value of embedding function at the equilibrium. In order to have an applicable EAM model, the embedding function $F(\rho)$, the atomic electron

density distribution $f(r)$, the two-body potential $\phi(r)$ and the modified term $M(P)$ must be determined. In this present model, the embedding function $F(\rho)$ is taken as the form [3], namely

$$F(\rho) = -F_0 \left[1 - \ln \left(\frac{\rho}{\rho_e} \right)^n \right] \left(\frac{\rho}{\rho_e} \right)^n \quad (14)$$

where the parameters F_0 and n are determined as follows:

$$F_0 = E_c = E_{1f} \quad (15)$$

$$n = \sqrt{\frac{\Omega B}{A \beta^2 E_{1f}}} \quad (16)$$

where E_c is the cohesive energy, β is the decay power of the atomic electron density distribution function. The electron density distribution function of an atom $f(r)$ is taken as [3].

$$f(r) = f_e \left(\frac{r_1}{r} \right)^\beta \quad (17)$$

where the parameter f_e determined in the present model is taken as [8].

$$f_e = \left(\frac{E_c - E_{1f}}{\Omega} \right)^{(3/5)} \quad (18)$$

and the model parameter β is empirically taken as “6” for metal and alloy.

Certainly, its exact values can be obtained by fitting (17) to the results of Clement and Roetti [9], the two-body potential function $\phi(r)$ is taken as by Quyang et al. [8].

$$\phi(r) = K_0 + K_1 \left(\frac{r}{r_1} \right)^2 + K_2 \left(\frac{r}{r_1} \right)^4 + K_3 \left(\frac{r}{r_1} \right)^{12} \quad (19)$$

$$K_0 = -\frac{1}{7} E_{1f} - 15 \Omega G \frac{10097924A + 12332488}{96(1238475A + 825650)} \quad (20)$$

$$K_1 = 15 \Omega G \frac{1633023A - 811174}{96(1238475A + 825650)} \quad (21)$$

$$K_2 = 15 \Omega G \frac{688128 - 137781A}{32(1238475A + 825650)} \quad (22)$$

$$K_3 = 15 \Omega G \frac{1024(2A - 1)}{1238475A + 825650} \quad (23)$$

As for the modified term, considering the two assumptions mentioned above, the real host electron density should be

$$\rho_{rel} = \rho + \Delta\rho \quad (24)$$

where ρ_{rel} is the electron density of the host obtained by the two assumptions, $\Delta\rho$ is the deviation; results from the assumption of spherical distribution of an atomic electron density and the assumption of linear superposition of an electron density. Substituting ρ_{rel} into (14), the energy change, which results from $\Delta\rho$, is

$$\Delta E(\Delta\rho) \propto -(\Delta\rho)^2 \quad (25)$$

Because $\Delta\rho$ is very small, then

$$\Delta E(\Delta\rho) \propto \text{Exp}[-(\Delta\rho)^2] \quad (26)$$

Baskes et al. [15], responded that the electron density change, $\Delta\rho$, results from the polarity could be expressed as

$$\Delta\rho \propto \sum_{j \neq i} f^2(r_{ij}) \quad (27)$$

From the above considerations and (12) and (13), let P represents the $\Delta\rho$ and P_e represents the average value of P , and then the modified term $M(P)$ is empirically taken as

$$M(P) = \alpha \left[\left(\frac{P}{P_e} - 1 \right)^2 \right] \exp \left[- \left(\frac{P}{P_e} - 1 \right)^2 \right] \quad (28)$$

This has only one parameter, α which can be determined from (11) and (16). Now the model parameters K_i ($i = 0, 1, 2, 3$), f_e , F_0 , n and α can be determined from the input physical parameters; a , E_c , E_{1f} , B , G and A with the above equations and only one adjustable parameter β is empirically taken as “6”, so the present model is complete. The input physical parameters are listed in Table 1, and the corresponding model parameters are listed in Table 2. In the present model, the two-body potential and

Table 1
Input physical parameters.

	Fe	Cr	V	Ta	Nb	Mo	W	Ref.
a (Å)	2.86645	2.8845	3.0399	3.3026	3.3008	3.15	3.16475	Frederikse [10]
E_C (eV)	4.29	4.10	5.3	8.089	7.47	6.81	8.66	Kittle [11]
E_{1f} (eV)	1.79	1.80	2.10	2.950	2.75	3.10	3.95	Maier et al. [12], Campbell and Schultz [13]
Ω_B (eV)	12.255	11.936	13.62	21.733	18.857	25.656	30.630	Hearmon [14]
Ω_G (eV)	6.555	8.688	4.17	7.961	4.409	12.290	15.829	Hearmon [14]
A	2.462	0.714	0.791	1.559	0.514	0.762	1.001	Hearmon [14]

Table 2
The model parameters determined from the input physical parameters.

	Fe	Cr	V	Ta	Nb	Mo	W
K_0	−0.348	1.463	0.445	0.006	0.763	1.836	1.538
K_1	−0.298	−3.162	−1.394	−1.174	−2.031	−4.213	−4.213
K_2	0.277	1.403	0.629	0.640	0.873	0.899	1.978
K_3	0.101	0.031	0.022	0.093	0.001	0.056	0.118
f_e	0.395	0.371	0.412	0.471	0.448	0.422	0.483
F_0	2.500	2.300	3.200	5.139	7.720	7.710	4.710
n	0.278	0.508	0.477	0.362	0.608	0.549	0.464
α	0.017	−0.154	0.117	0.180	0.141	0.022	0.006
β	6	6	6	6	6	6	6

the electron density functions should have a cut-off. A cubic spline function is used as a cut-off function. The cut-off procedure is the same as that used by Bangwei and Yifang [5] with the start point ($r_s = r_2$) and the end point ($r_c = \sqrt{2}r_2$).

Fig. 1, shows the two-body potentials of Fe, V and Cr and Fig. 2, shows the typical atomic electron density function after the cut-off procedure applied. The present potential is similar to that of Johnson and Oh [4] with stiffness within the nearest-neighbor, and is better than that of Pasianot et al. [6] especially for Cr. Fig. 3, shows a typical embedding function, which is the same as that of Johnson [3].

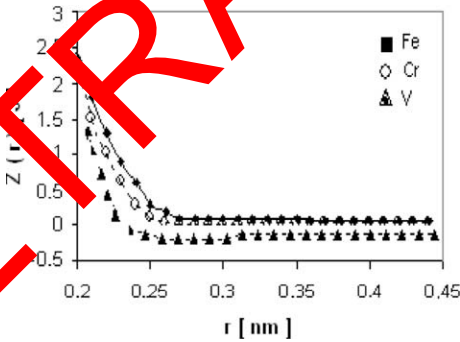


Fig. 1. The curves of two-body potentials for Fe, Cr and V.

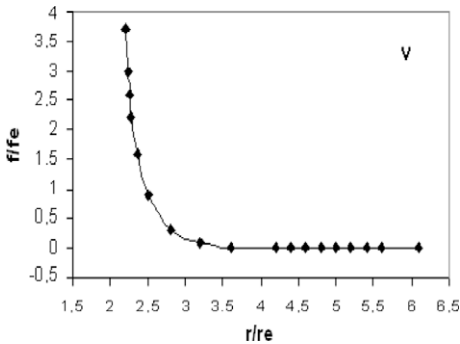


Fig. 2. A typical curve of atomic density distribution function.

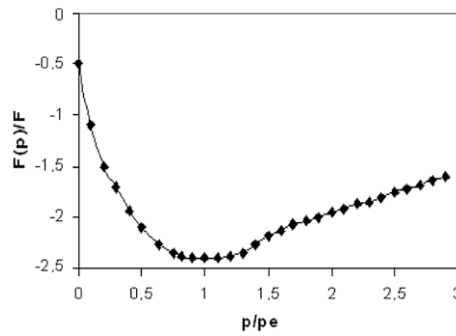


Fig. 3. A typical curve of embedding function.

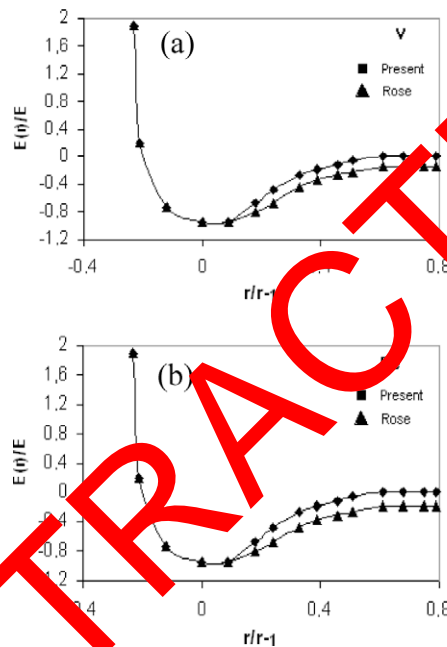


Fig. 4. A typical curve of total energy of the present model (solid line) and the results of Rose's equation for V (a) and Fe (b).

The comparison of the curve of total energy for the present model and Rose equation are shown in Fig. 4 for V (a) and Fe (b). From the figure, it can be seen that the agreement between them is good. When the model is applied to study the properties of an alloy, the interaction potential between different types of atoms must be defined here, so the Johnson and Oh [4] form is taken:

$$\phi^{ab}(r) = \frac{1}{2} \left[\frac{f^a(r)}{f^b(r)} \phi^{bb}(r) + \frac{f^b(r)}{f^a(r)} \phi^{aa}(r) \right] \quad (29)$$

where a and b indicate the types of atoms.

3. Results and discussion

3.1. The dilute solution enthalpies

The present analytical EAM is applied to calculate the dilute solution enthalpies of the binary alloys of bcc metals; Fe, Cr and V. The calculated procedure is similar to that described in details in [5]. The only difference between the EAM and this model is that there is an extra modified term in the equation of the total energy in our present model. The comparison of the calculated dilute solution enthalpies to the available experimental data is shown in Fig. 5. From the figure, it can be seen that the calculated values are in good agreement with those of the available experiments. For the Fe–Cr system, the present

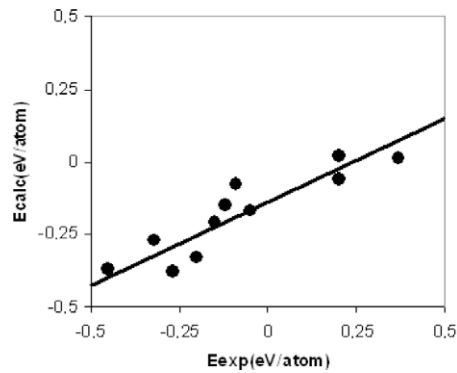


Fig. 5. The comparison of calculated dilute solution enthalpies with available experimental data [5].

results deviate from the experiment but the trend is similar. For all Fe-bearing alloys, the calculations are contrary to the results of Johnson's model [3].

In this paper, the solution enthalpies for Fe-bearing alloys are calculated, which cannot be calculated within Johnson's model because the model cannot describe the metal Fe. From Table 3 and Fig. 5, we can see that the present calculated results are in good agreement with the available experimental data except the system Fe–Fe for which discrepancy between the calculations and the experiments is large. For simplicity, the relaxation is not considered. The relaxation must affect the dilute solution enthalpy because of the difference in the distances between the solute and solvent atoms. This is one of the reasons caused this discrepancy between the calculation and the experiment. The other reason may be the factor of temperature. The results of calculations are at 0 K but the experimental data were obtained at nonzero temperature. The complete comparison of the calculated values to the experimental data is impossible because of the limited experimental data. From the discussions above, we can see that the present calculations for the dilute solution enthalpy are reasonably correct.

3.2. The formation enthalpies

The calculated formation enthalpies (solid curve) of the disordered alloys with any compositions for 4 binary alloys of three bcc transition metals are shown in Fig. 6. The following symbols stand for (▲) present results, (■) the results of first-principles calculation [19], (○) the available experimental data and (×) the results of Miedema et al. [20].

The results of Mo–Nb, Mo–Ta and Ta–W system are in agreement with the available experimental data and the calculated values of Colinet et al. [19] of Sigli et al. [11] and of Miedema et al. [20], respectively (see Table 3). The phase diagrams for the three alloy systems are all series solid solution and the structure of alloy in whole composition range is bcc, which is consistent with our assumption. On the other hand, the percentages of the rate of the discrepancy and the lattice constants of the two alloys constituents to the lattice constant, $\Delta a/a$ %, for these systems are less than 5%, and the elastic distortion energies are very small and have a little influence on alloying. As shown in Table 3, calculated values for Ta–W system

Table 3
The calculated dilute solution enthalpies and available experimental data, in (eV/atom).

Solvent	Solute						
	Fe	W	Mo	Cr	Ta	Nb	V
Fe		0.60	0.31	0.0001 0.22 ^a	−0.64	−0.97	−0.11 −0.16 ^a
W	0.61		0.06	0.40	−0.32 −0.22 c	−0.27 −0.27 ^b	0.35
Mo	0.35	0.06		0.19 0.21 ^a	−0.42	−0.40 −0.27 ^b	0.13
Cr	0.001 0.2 ^a	0.25	0.11 0.33 ^a		−1.23	−1.45	−0.17 −0.19 ^a
Ta	0.14	−0.29 −0.31 ^c	−0.39	−0.06		0.007	−0.17
Nb	0.15	−0.20	−0.33 −0.42 ^d	−0.03	0.005		−0.16
V	−0.02 −0.10 ^d	0.44	0.19	−0.12 −0.09 ^a	−0.11	−0.25	

^a Kubaschewski et al. [16].

^b Singhal and Worrell [17].

^c Colinet et al. [19].

^d Singhal and Worrell [18].

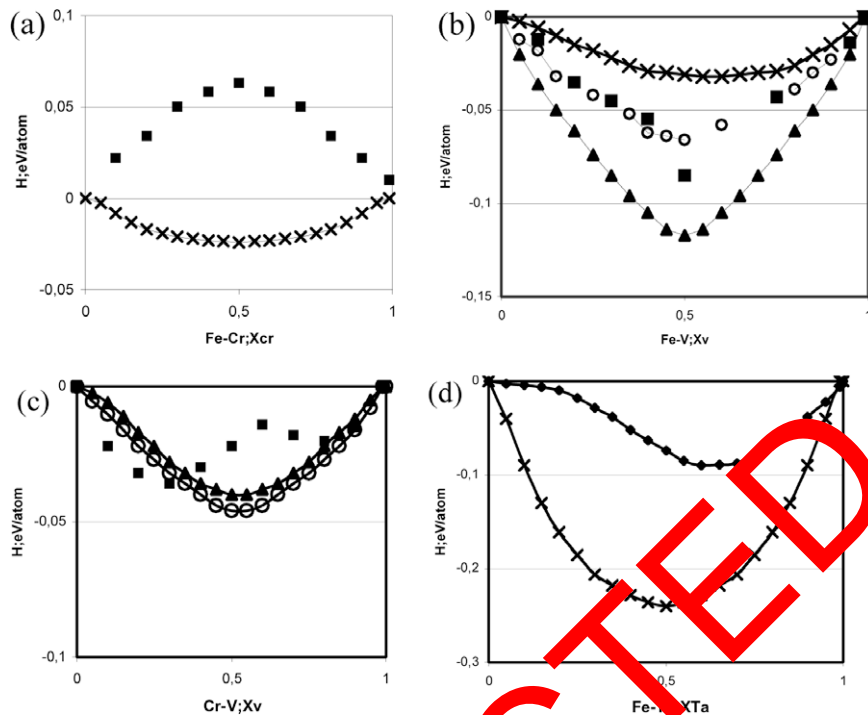


Fig. 6. The calculated formation enthalpies of random alloys in whole composition range. The following symbols stand for (\blacktriangle) present results, (\blacksquare) the results of first-principles calculation Colinet et al. [19], (\circ) the available experimental data and (\times) the results of Miedema et al. [20].

are in agreement with available data [3], calculated values shown in Table 3 for Fe–V system is in consistent the finding of Kubaschewski et al. [16]. Asymmetric view of the experimental data with the findings of Spencer and Putland [22] is an indication of compatibility of the two sets of data. The magnitude of present results is smaller than the results of experimental values. However the values calculated with Miedema's theory are larger in magnitude than the experimental data. For the experimental data, the results from different groups are different. In this paper, we use the results of Kubaschewski et al. [16] because the reference states, the element and the structure of alloy are bcc. Experiment of Kubaschewski et al. [16] is consistent with our assumption. The percentage of $\Delta a/a$ for Fe–V system is less than 6%, but the phase diagram of this system is not a solid series in whole composition range at low temperature.

The existence of σ phase makes the bcc structure assumption in the whole composition range for the present calculations, deviation from the fact. On the other hand, the present calculation without the temperature dependence may be considered as the results of room temperature, while the experimental data were measured at 1665 K. The factors mentioned above affect the results, and create a discrepancy. Chromium-bearing systems include Fe–Cr, Cr–V. From the phase diagrams of the two systems Cr–V is solid solution, and $\Delta a/a$ % of component for the system is less than 10%. Calculated values shown in Fe–Cr (Fig. 6(a)) and Cr–V (Fig. 6(c)), for systems are consistent with previous finding.

For Cr–V system, the results of are consistent with the present calculations. Fe–Cr has similar complexity in the phase diagrams. The present calculations and those of Colinet et al. [19] for Fe–Cr system indicate that the formation enthalpies are very small, and both of them are less than the experimental data which may result from the existence of σ phase as discussed in Fe–V system. The present results are in agreement with those of Colinet et al. [19]. The formation enthalpies for Cr–V system are in good agreement with those of Miedema et al. [20] (Fig. 6(c)). It can be seen that the curve of formation enthalpy is not symmetric and the lowest value is close to the value obtained for Cr. The present result of Fe–Ta system is in agreement with available data [20] (Fig. 6(d)). From the above discussions, we can see that the present results are consistent with those of the experiments or the results of first-principles calculation [20] or thermodynamic calculations. We may conclude that the present analytical EAM is successful in the calculations of thermodynamic properties for all of the transition bcc metals including Fe.

4. Conclusions

A simple analytical EAM model for the bcc metals has been developed. In the new model, a modified term of energy was introduced to fit the negative Cauchy pressure of Fe, and a new form of two-body potential was also proposed. This potential function can represent the interaction between the atoms in a wide range. The introduction of new modified term has a potential to overcome some of the problems faced with implementation of the EAM method, which excluded Fe metal in the

previous studies. All parameters of the model have been determined. The calculated dilute solution enthalpies are in good agreement with the available experimental data. The formation enthalpies are in good agreement with the available experimental data and those of the first principles calculations. As a result, the present model is generally in good agreement with Miedema's theory.

References

- [1] Daw MS, Baskes MI. Phys Rev B 1984;29:6443.
- [2] Bangwei Z, Yifang OY, Shuzi L, Zhanpeng J. Physica B 1996;101:161–8.
- [3] Johnson RA. Phys Rev B 1973;39:12554.
- [4] Johnson RA, Oh DJ. J Mater Res 1989;4:1195.
- [5] Bangwei Z, Yifang OY. Phys Rev B 1993;48:3022.
- [6] Pasianot R, Farkas D, Savino EJ. Phys Rev B 1991;43:6952.
- [7] Adams JB, Foiles SM. Phys Rev B 1990;41:3361.
- [8] Quyang Y, Zhang B, Liao S, Z Jin: Z Phys B 1996;101:161–8.
- [9] Clementi E, Roetti C. Data Nucl. Data Tables 1974;14:3–4.
- [10] Frederikse HPR. American institute of physics hand-book. New York: McGraw-Hill; 1972.
- [11] Kittle C. Introduction to solid state physics. New York: Wiley; 1976.
- [12] Maier K, Peo M, Saile B, Schaefer HE, Seeger A. Philos Mag A 1991;40:701.
- [13] Campbell JL, Schultz CW. Appl Phys 1979;19:149.
- [14] Hearmon RFS. Londolt–Börnstein. New Series Iii/18. Berlin, Heidelberg, New York: Springer; 1983.
- [15] Baskes MI, Nelson JS, Wright AF. Phys Rev B 1989;40:6085.
- [16] Kubaschewski O, Probst H, Geioer KH. Z Phys Chem Neue Folge 1977;104:23.
- [17] Singhal SC, Worrell WL. Metall Trans 1973;4:1125.
- [18] Singhal SC, Worrell WL. Metall Trans 1973;4:895.
- [19] Colinet C, Beesound A, Pasturel A. J Phys F: Met Phys 1988;18:903.
- [20] Miedema AR, de Chatel PF, de Boer FR. Physica B 1980;100:1.
- [21] Sigli C, Kosugi M, Sanchez JM. Phys Rev Lett 1986;57:253.
- [22] Spencer PJ, Putland FH. J. Iron Stell Inst 1973;211:293.

RETRACTED